



ARTICLE

Exact Run Length Evaluation on a Two-Sided Modified Exponentially Weighted Moving Average Chart for Monitoring Process Mean

Piyatida Phanthuna, Yupaporn Areepong* and Saowanit Sukparungsee

Department of Applied Statistics, King Mongkut's University of Technology North Bangkok, Bangkok, 10800, Thailand

*Corresponding Author: Yupaporn Areepong. Email: yupaporn.a@sci.kmutnb.ac.th

Received: 22 August 2020 Accepted: 09 December 2020

ABSTRACT

A modified exponentially weighted moving average (EWMA) scheme is one of the quality control charts such that this control chart can quickly detect a small shift. The average run length (ARL) is frequently used for the performance evaluation on control charts. This paper proposes the explicit formula for evaluating the average run length on a two-sided modified exponentially weighted moving average chart under the observations of a first-order autoregressive process, referred to as AR(1) process, with an exponential white noise. The performance comparison of the explicit formula and the numerical integral technique is carried out using the absolute relative change for checking the correct formula and the CPU time for testing speed of calculation. The results show that the ARL of the explicit formula and the numerical integral equation method are hardly different, but this explicit formula is much faster for calculating the ARL and offered accurate values. Furthermore, the cumulative sum, the classical EWMA and the modified EWMA control charts are compared and the results show that the latter is better for small and intermediate shift sizes. In addition, the explicit formula is successfully applied to real-world data in the health field as COVID-19 data in Thailand and Singapore.

KEYWORDS

Explicit formula; average run length; modified EWMA chart; AR(1) process; exponential white noise

1 Introduction

Statistical analysis is important for confirming consistency and has received interest from many business areas requiring increased reliability. In the manufacturing industry, statistical process control is used extensively and a control chart is one of the quality control tools and has been applied in many fields such as finance [1], health [2] and medicine [3]. In 1924, Shewhart created the first control chart which can detect a large-sized process shift quickly [4]. Next, the exponentially weighted moving average (EWMA) chart [5] and the cumulative sum (CUSUM) chart [6] were developed and found to be faster for small shift detection. In addition, other new control charts have been developed, one of which is the modified EWMA control chart. Patel et al. [7] expanded the modified EWMA control chart from a fusion of the characteristics of the Shewhart and EWMA control charts that could detect a small size shift quickly and was more effective for autocorrelated data. The modified EWMA statistic is based on the classical



EWMA statistic by using past observations with additional consideration of changes in the recent past for pairs of observations in the process. Next, Khan et al. [8] increased the performance of the modified EWMA scheme by maintaining a constant r in the last term of the modified EWMA statistic.

The average run length (ARL) [9] is the average number of in-control observations before an out-of-control signal occurs and is classified based on two stages: ARL at the initial mean (ARL_0) and ARL when the process mean has shifted (ARL_1). It is now a popular performance measure for a control chart and has been frequently used for research evaluation with many methods, such as Monte Carlo simulation, a Markov Chain approach, a Martingale approach, a numerical integral equation (NIE), and an explicit formula. All of these methods can be used to approximate the ARL but only the last one can be calculated using the least time and obtained the accuracy ARL. For research examples, Flury et al. [10] simulated the ARL to evaluate the multivariate EWMA control chart performance with highly asymmetric gamma distributions. The Markov Chain approach was used by Chanant et al. [11] for the ARL evaluation of EWMA and CUSUM control charts based on the zero-inflated negative binomial (ZINB) model. The Martingale approach was predicated by Sukparungsee [12] to approximate the ARL with optimal parameters of one and two-sided EWMA control chart.

There are many examples in the literature of using the explicit formula and the NIE method for the ARL on control charts. First, Suriyakat et al. [13] presented an explicit formula and a numerical method to solve the ARL on an EWMA control chart for a first-order autoregressive (AR(1)) process with an exponential white noise. Meanwhile, Busaba et al. [14] proposed numerical approximations of ARL on a CUSUM chart for an AR(1) model with exponential white noise. Next, Pecharat et al. [15] derived an explicit formula and a numerical integration scheme for the ARL on a CUSUM control chart for a moving average process of order q (MA(q)) with an exponential white noise. Later, Peerajit et al. [16] solved the NIEs for the ARL for a long memory process with non-seasonal and seasonal autoregressive fractionally integrated moving average (ARFIMA) models on a CUSUM control chart. After that, Sukparungsee et al. [17] analyzed explicit formulas of the ARL for an EWMA control chart using an autoregressive model. Moreover, Sunthornwat et al. [18] reported an explicit formula and a numerical technique to find the ARL on an EWMA control chart for a long memory ARFIMA process, and also presented the evaluation of ARL of an EWMA control chart for a long memory ARFIMA process with optimal parameters [19]. Recently, Peerajit et al. [20] introduced the ARL evaluation for CUSUM chart on a seasonal autoregressive fractionally integrated moving average (SARFIMA) process with an exponential white noise by using explicit analytical solutions.

Autoregressive models are often used on control charts in the recent literature [21–23]. The order of an autoregressive model is the number of immediate previous values used to predict the present value. A first-order autoregressive model considered in this research is an appropriate process for numerous data sources in real life such as environmental [24], physical [25] and industrial [26] data. Moreover, the modified EWMA control chart can be effectively used with an autocorrelated data.

In this paper, we present the explicit formula to evaluate the ARL on a two-sided modified EWMA control chart for the AR(1) process with an exponential white noise, which is the error term with an exponential distribution that has been studied recently [27–29]. In the next section, the AR(1) process features are shown and applied to a modified EWMA scheme. Following this, the ARL is calculated using the explicit formula and the NIE method, and after that, the

performance of the schemes to detect shifts between the CUSUM, the classical EWMA and the modified EWMA control charts with simulated and real-world data are reported and compared.

2 Control Chart and Process

2.1 Classical and Modified EWMA Control Charts

The modified exponentially weighted moving average (EWMA) control chart introduced by Patel et al. [7] and Khan et al. [8] were adjustments of the classical EWMA scheme. Let $\{X_t\}$ for $t = 1, 2, 3, \dots$ be a sequence of random variables on the AR(1) process with mean μ and variance σ^2 , and λ is an exponential smoothing parameter, where $0 < \lambda < 1$. The modified EWMA statistic with adjusted constant r is expressed as:

$$Z_t = (1 - \lambda)Z_{t-1} + \lambda X_t + r(X_t - X_{t-1}); \quad t = 1, 2, 3, \dots \quad (1)$$

and the asymptotic variance of Z_t is $\left(\frac{\lambda + 2\lambda r + 2r^2}{2 - \lambda}\right)\sigma^2$. From Eq. (1), we can show that

- (1) If $r = 0$, the classical EWMA statistic coincides with $Z_t = (1 - \lambda)Z_{t-1} + \lambda X_t$.
- (2) If $r = 1$, the primal modified EWMA statistic coincides with $Z_t = (1 - \lambda)Z_{t-1} + \lambda X_t + (X_t - X_{t-1})$.

The upper and lower control limits of the classical EWMA control chart are:

$$\mu \pm L\sigma \sqrt{\frac{\lambda}{2 - \lambda}} \quad (2)$$

and the bound control limits of the modified EWMA control chart are:

$$\mu \pm L_m\sigma \sqrt{\frac{\lambda + 2\lambda r + 2r^2}{2 - \lambda}} \quad (3)$$

where μ is the process mean, σ is the process standard deviation and L and L_m are suitable control width limits.

2.2 CUSUM Control Chart

The cumulative sum (CUSUM) chart has been widely used to detect small shifts similar to the EWMA chart on the control process and was initially proposed by Page [6]. Let $\{X_t\}$ for $t = 1, 2, 3, \dots$ be a sequence of random variables on the AR(1) process with mean μ and variance σ^2 . The upper CUSUM statistic can be expressed by:

$$Z_t = \max\{0, Z_{t-1} + X_t - q\}; \quad t = 1, 2, 3, \dots \quad (4)$$

where q is usually called a reference value or a constant of CUSUM chart, $Z_0 = u$ is an initial value with $u \in [0, b]$ and b is an upper control limit (UCL).

2.3 Modified EWMA Chart for the AR(1) Process

The equation of observations for the AR(1) process in the case of an exponential white noise is defined as:

$$X_t = \eta + \phi X_{t-1} + \varepsilon_t \quad (5)$$

where X_t ($t = 1, 2, 3, \dots$) is a sequence of random variables, η is a suitable constant, ϕ is an autoregressive coefficient ($|\phi| < 1$), and ε_t denotes white noise sequences of the exponential distribution ($\varepsilon_t \sim \text{Exp}(\beta)$).

The modified EWMA statistic under the upper bound assumption for the AR(1) process substituted from Eq. (5) into Eq. (1) can be arranged by recursion:

$$\begin{aligned} Z_t &= (1 - \lambda) Z_{t-1} + \lambda X_t + r(X_t - X_{t-1}) \\ Z_t &= (1 - \lambda) Z_{t-1} + \lambda(\eta + \phi X_{t-1} + \varepsilon_t) + r(\eta + \phi X_{t-1} + \varepsilon_t - X_{t-1}) \\ Z_t &= (1 - \lambda) Z_{t-1} + (\lambda\phi + r\phi - r) X_{t-1} + (r + \lambda) \varepsilon_t + (r + \lambda) \eta \end{aligned} \quad (6)$$

where $Z_0 = u$ is the initial value. Therefore,

$$Z_t = (1 - \lambda) u + (\lambda\phi + r\phi - r) X_{t-1} + (r + \lambda) \varepsilon_t + (r + \lambda) \eta.$$

The corresponding stopping time for detecting an out-of-control process on a two-sided modified EWMA control chart can be written as:

$$\tau_{a,b} = \inf \{t > 0; Z_t < a \text{ or } Z_t > b\}, \quad a \leq u \leq b \quad (7)$$

where a is the lower control limit and b is the upper control limit. If Z_t is in an in-control process and substituted with the term of ε_t , then

$$\begin{aligned} a &\leq Z_t \leq b \\ a &\leq (1 - \lambda) u + (\lambda\phi + r\phi - r) X_{t-1} + (r + \lambda) \varepsilon_t + (r + \lambda) \eta \leq b \\ \frac{a - (1 - \lambda) u - (\lambda\phi + r\phi - r) X_{t-1}}{(r + \lambda)} - \eta &\leq \varepsilon_t \leq \frac{b - (1 - \lambda) u - (\lambda\phi + r\phi - r) X_{t-1}}{(r + \lambda)} - \eta. \end{aligned} \quad (8)$$

The ARL of the modified EWMA control chart with the AR(1) model is given by:

$$\text{ARL} = E_\theta (\tau_{a,b}) \quad (9)$$

where θ is the change-point time, $E_\theta(\cdot)$ is the expectation under the assumption that the change-point occurs at time θ .

3 Integral Equation Method for Solving ARL

For analytical solutions, the ARL on the modified EWMA control chart with the AR(1) model is developed under the condition of a unique integral equation. $L(u)$ is defined for an initial ARL and $L(u) = E_\infty(\tau_{a,b})$. In accordance with the method of Champ et al. [30], $L(u)$ can be found as:

$$L(u) = 1 + \int_{\frac{a - (1 - \lambda) u - (\lambda\phi + r\phi - r) X_{t-1}}{(r + \lambda)} - \eta}^{\frac{b - (1 - \lambda) u - (\lambda\phi + r\phi - r) X_{t-1}}{(r + \lambda)} - \eta} L[(1 - \lambda) u + (\lambda\phi + r\phi - r) X_{t-1} + (r + \lambda) y + (r + \lambda) \eta] f(y) dy.$$

If $k = (1 - \lambda) u + (\lambda\phi + r\phi - r) X_{t-1} + (r + \lambda) y + (r + \lambda) \eta$ is defined for changing the variable of integration, then $L(u)$ is transformed as:

$$L(u) = 1 + \frac{1}{r + \lambda} \int_a^b L(k) f\left(\frac{k - (1 - \lambda) u - (\lambda\phi + r\phi - r) X_{t-1}}{(r + \lambda)} - \eta\right) dk. \quad (10)$$

Since $f(y) = \frac{1}{\beta} e^{-\frac{y}{\beta}}$; $y \geq 0$, then

$$L(u) = 1 + \frac{e^{\frac{(1-\lambda)u}{\beta(r+\lambda)}} \cdot e^{\frac{(\lambda\phi+r\phi-r)X_{t-1}}{\beta(r+\lambda)}} \cdot e^{\frac{\eta}{\beta}}}{\beta(r+\lambda)} \int_a^b L(k) \cdot e^{\frac{-k}{\beta(r+\lambda)}} dk. \tag{11}$$

From Eq. (11), the existence and uniqueness of the solutions for the integral equation are proved by the mathematical theory. The integral equation for solving the ARL on the modified EWMA chart with the AR(1) process is proved that can be existed and has a unique solution by using Banach’s fixed point theory [31].

Theorem 1: Let X be a complete metric space $(V, \|\cdot\|)$. If Λ is a contraction mapping whereby $\Lambda: X \rightarrow X$, then Λ has a unique fixed point x .

Theorem 2: Let X be a complete metric space $(V, \|\cdot\|)$. $\Lambda: X \rightarrow X$ is a contraction mapping if L is any vector in X and Λ has a Lipschitz constant $c \in [0, 1)$ such that $L = \lim_{n \rightarrow \infty} \Lambda(L_n)$ and

$$\|\Lambda(L_g) - \Lambda(L_h)\| \leq c \|L_g - L_h\| \quad \text{for all } L_g, L_h \in X. \tag{12}$$

Proof: For a first part, let Λ be a contraction mapping in the complete metric space $(V, \|\cdot\|)$ when $L_0 \in V$, and define a sequence $\{L_n\}_{n \in \mathbb{N}}$ given by $L_{n+1} = \Lambda(L_n)$ for $n \geq 0$. Show that $L = \lim_{n \rightarrow \infty} \Lambda(L_n)$ such that $\{L_n\}_{n \in \mathbb{N}}$ is supposed to be Cauchy sequence, so

$$\|L_{n+1} - L_n\| = \|\Lambda(L_n) - \Lambda(L_{n-1})\| \leq c \|L_n - L_{n-1}\| \leq c^n \|L_1 - L_0\|$$

where $\|L_1 - L_0\|$ is a finite number. After that, using this solution and the triangle inequality for all $m > n \geq N$ can be solved as:

$$\|L_{n+m} - L_n\| \leq \sum_{i=0}^{m-1} c^{n+i} \|L_1 - L_0\| \leq \frac{c^n}{1-c} \|L_1 - L_0\| < \varepsilon,$$

where $\varepsilon > 0$ and $c \in [0, 1)$. Therefore, the sequence $\{L_n\}_{n \in \mathbb{N}}$ is a Cauchy such that:

$$\Lambda(L) = \Lambda\left(\lim_{n \rightarrow \infty} L_n\right) = \lim_{n \rightarrow \infty} \Lambda(L_n) = \lim_{n \rightarrow \infty} L_{n+1} = L.$$

Thus, L is called a fixed point of Λ .

Next part has to show that this fixed point is unique. Given $L_g, L_h \in V$ in the complete metric space $(V, \|\cdot\|)$ for all $u \in [a, b]$, then Eqs. (11) and (12) are considered as:

$$\begin{aligned} \|\Lambda(L_g) - \Lambda(L_h)\|_\infty &= \sup_{u \in [a, b]} |L_g(u) - L_h(u)| \\ \|\Lambda(L_g) - \Lambda(L_h)\|_\infty &\leq \sup_{u \in [a, b]} \left\{ \|L_g - L_h\|_\infty \frac{e^{\frac{(1-\lambda)u}{\beta(r+\lambda)}} \cdot e^{\frac{(\lambda\phi+r\phi-r)X_{t-1}}{\beta(r+\lambda)}} \cdot e^{\frac{\eta}{\beta}}}{\beta(r+\lambda)} \left| \int_a^b e^{\frac{-k}{\beta(r+\lambda)}} dk \right| \right\} \\ \|\Lambda(L_g) - \Lambda(L_h)\|_\infty &= \sup_{u \in [a, b]} \left\{ e^{\frac{(1-\lambda)b}{\beta(r+\lambda)}} \cdot e^{\frac{(\lambda\phi+r\phi-r)X_{t-1}}{\beta(r+\lambda)}} \cdot e^{\frac{\eta}{\beta}} \left(e^{\frac{-a}{\beta(r+\lambda)}} - e^{\frac{-b}{\beta(r+\lambda)}} \right) \right\} \|L_g - L_h\|_\infty \\ \|\Lambda(L_g) - \Lambda(L_h)\|_\infty &\leq c \|L_g - L_h\|_\infty. \end{aligned}$$

Hence, $\|\Lambda(L_g) - \Lambda(L_h)\|_\infty \leq c \|L_g - L_h\|_\infty$, where positive constant $c \in [0, 1)$ and Λ is the contraction mapping on a complete metric space $(V, \|\cdot\|)$. Therefore, the integral equation for solving of ARL on the modified EWMA chart with the AR(1) process has a unique solution.

4 Explicit Formula for ARL

The explicit analytical solutions of the ARL on the modified EWMA control chart with the AR(1) model constructed after checking for unique solutions are:

$$L(u) = 1 - \frac{\lambda e^{\frac{(1-\lambda)u}{\beta(r+\lambda)}} \left(e^{\frac{-b}{\beta(r+\lambda)}} - e^{\frac{-a}{\beta(r+\lambda)}} \right)}{\lambda e^{-\frac{(\lambda\phi+r\phi-r)X_{t-1}+(r+\lambda)\eta}{\beta(r+\lambda)}} + e^{\frac{-\lambda b}{\beta(r+\lambda)}} - e^{\frac{-\lambda a}{\beta(r+\lambda)}}}. \quad (13)$$

Proof: In the first step, the solution of Eq. (11) as: $L(u) = 1 + \frac{e^{\frac{(1-\lambda)u}{\beta(r+\lambda)}} \cdot e^{\frac{(\lambda\phi+r\phi-r)X_{t-1}}{\beta(r+\lambda)}} \cdot e^{\frac{\eta}{\beta}}}{\beta(r+\lambda)}$

$\int_a^b L(k) \cdot e^{\frac{-k}{\beta(r+\lambda)}} dk$ is determined as: $D = \int_a^b L(k) \cdot e^{\frac{-k}{\beta(r+\lambda)}} dk$ which is a constant and $C(u) = e^{\frac{(1-\lambda)u}{\beta(r+\lambda)}} \cdot e^{\frac{(\lambda\phi+r\phi-r)X_{t-1}}{\beta(r+\lambda)}} \cdot e^{\frac{\eta}{\beta}}$; $a \leq u \leq b$ such that it can be rewritten as:

$$L(u) = 1 + \frac{C(u)}{\beta(r+\lambda)} \cdot D. \quad (14)$$

Consider D and take turns $L(k)$ with Eq. (14), then

$$\begin{aligned} D &= \int_a^b L(k) \cdot e^{\frac{-k}{\beta(r+\lambda)}} dk \\ D &= \int_a^b \left(1 + \frac{C(k)}{\beta(r+\lambda)} \cdot D \right) e^{\frac{-k}{\beta(r+\lambda)}} dk \\ D &= \int_a^b e^{\frac{-k}{\beta(r+\lambda)}} dk + \int_a^b \frac{C(k)}{\beta(r+\lambda)} \cdot D \cdot e^{\frac{-k}{\beta(r+\lambda)}} dk \\ D &= -\beta(r+\lambda) \left[e^{\frac{-b}{\beta(r+\lambda)}} - e^{\frac{-a}{\beta(r+\lambda)}} \right] - \frac{D}{\lambda} \cdot e^{\frac{(\lambda\phi+r\phi-r)X_{t-1}}{\beta(r+\lambda)}} \cdot e^{\frac{\eta}{\beta}} \left[e^{\frac{-\lambda b}{\beta(r+\lambda)}} - e^{\frac{-\lambda a}{\beta(r+\lambda)}} \right] \\ D &= \frac{-\beta(r+\lambda) \left[e^{\frac{-b}{\beta(r+\lambda)}} - e^{\frac{-a}{\beta(r+\lambda)}} \right]}{1 + \frac{1}{\lambda} \cdot e^{\frac{(\lambda\phi+r\phi-r)X_{t-1}}{\beta(r+\lambda)}} \cdot e^{\frac{\eta}{\beta}} \left[e^{\frac{-\lambda b}{\beta(r+\lambda)}} - e^{\frac{-\lambda a}{\beta(r+\lambda)}} \right]}. \end{aligned} \quad (15)$$

Finally, by substituting constant D from Eq. (15) into Eq. (14), then $L(u)$ can be found:

$$\begin{aligned} L(u) &= 1 + \frac{C(u)}{\beta(r+\lambda)} \cdot D \\ L(u) &= 1 + \frac{e^{\frac{(1-\lambda)u}{\beta(r+\lambda)}} \cdot e^{\frac{(\lambda\phi+r\phi-r)X_{t-1}}{\beta(r+\lambda)}} \cdot e^{\frac{\eta}{\beta}}}{\beta(r+\lambda)} \left(\frac{-\beta(r+\lambda) \left[e^{\frac{-b}{\beta(r+\lambda)}} - e^{\frac{-a}{\beta(r+\lambda)}} \right]}{1 + \frac{1}{\lambda} \cdot e^{\frac{(\lambda\phi+r\phi-r)X_{t-1}}{\beta(r+\lambda)}} \cdot e^{\frac{\eta}{\beta}} \left[e^{\frac{-\lambda b}{\beta(r+\lambda)}} - e^{\frac{-\lambda a}{\beta(r+\lambda)}} \right]} \right) \end{aligned}$$

$$L(u) = 1 - \frac{\lambda e^{\frac{(1-\lambda)u}{\beta(r+\lambda)}} \cdot e^{\frac{(\lambda\phi+r\phi-r)X_{t-1}}{\beta(r+\lambda)}} \cdot e^{\frac{\eta}{\beta}} \left[e^{\frac{-b}{\beta(r+\lambda)}} - e^{\frac{-a}{\beta(r+\lambda)}} \right]}{\lambda + e^{\frac{(\lambda\phi+r\phi-r)X_{t-1}}{\beta(r+\lambda)}} \cdot e^{\frac{\eta}{\beta}} \left[e^{\frac{-\lambda b}{\beta(r+\lambda)}} - e^{\frac{-\lambda a}{\beta(r+\lambda)}} \right]}$$

$$L(u) = 1 - \frac{\lambda e^{\frac{(1-\lambda)u}{\beta(r+\lambda)}} \left[e^{\frac{-b}{\beta(r+\lambda)}} - e^{\frac{-a}{\beta(r+\lambda)}} \right]}{\lambda e^{-\frac{(\lambda\phi+r\phi-r)X_{t-1}}{\beta(r+\lambda)}} \cdot e^{-\frac{\eta}{\beta}} + \left[e^{\frac{-\lambda b}{\beta(r+\lambda)}} - e^{\frac{-\lambda a}{\beta(r+\lambda)}} \right]}$$

$$L(u) = 1 - \frac{\lambda e^{\frac{(1-\lambda)u}{\beta(r+\lambda)}} \left(e^{\frac{-b}{\beta(r+\lambda)}} - e^{\frac{-a}{\beta(r+\lambda)}} \right)}{\lambda e^{-\frac{(\lambda\phi+r\phi-r)X_{t-1}+(r+\lambda)\eta}{\beta(r+\lambda)}} + e^{\frac{-\lambda b}{\beta(r+\lambda)}} - e^{\frac{-\lambda a}{\beta(r+\lambda)}}}.$$

Therefore, the solution to Eq. (13) is obtained.

For an in-control process, the exponential parameter is set to $\beta = \beta_0$ and the explicit formula with β_0 called ARL_0 can be written as:

$$ARL_0 = 1 - \frac{\lambda e^{\frac{(1-\lambda)u}{\beta_0(r+\lambda)}} \left(e^{\frac{-b}{\beta_0(r+\lambda)}} - e^{\frac{-a}{\beta_0(r+\lambda)}} \right)}{\lambda e^{-\frac{(\lambda\phi+r\phi-r)X_{t-1}+(r+\lambda)\eta}{\beta_0(r+\lambda)}} + e^{\frac{-\lambda b}{\beta_0(r+\lambda)}} - e^{\frac{-\lambda a}{\beta_0(r+\lambda)}}}. \tag{16}$$

On the other hand, the exponential parameter for an out-of-control process is defined as $\beta_1 = (1 + \delta)\beta_0$, where $\beta_1 > \beta_0$ and δ is the shift size such that the explicit formula of β_1 can be described as:

$$ARL_1 = 1 - \frac{\lambda e^{\frac{(1-\lambda)u}{\beta_1(r+\lambda)}} \left(e^{\frac{-b}{\beta_1(r+\lambda)}} - e^{\frac{-a}{\beta_1(r+\lambda)}} \right)}{\lambda e^{-\frac{(\lambda\phi+r\phi-r)X_{t-1}+(r+\lambda)\eta}{\beta_1(r+\lambda)}} + e^{\frac{-\lambda b}{\beta_1(r+\lambda)}} - e^{\frac{-\lambda a}{\beta_1(r+\lambda)}}}. \tag{17}$$

5 Numerical Method for Solving the Integral Equation

The NIE method is used to solve the ARL for the AR(1) process of the two-sided modified EWMA control chart in Eq. (10). The ARL solution or $L_{NIE}(u)$ is approximated with the m linear equation systems over the interval $[a, b]$ by using the composite midpoint quadrature rule [32]. This NIE method is proposed for the two-sided modified EWMA control chart by using the length of m equal divided intervals $w_j = \frac{b-a}{m}$ and the middle point of the j^{th} interval $x_j = \left(j - \frac{1}{2}\right)w_j + a$.

Therefore, the ARL solution of the NIE method can be rewritten as:

$$L_{NIE}(u) \approx 1 + \frac{1}{r+\lambda} \sum_{j=1}^m w_j L(x_j) f\left(\frac{x_j - (1-\lambda)u - (\lambda\phi+r\phi-r)X_{t-1}}{(r+\lambda)} - \eta\right). \tag{18}$$

6 Comparison of the ARL Results

In this section, the performances of the explicit formula and the NIE method are compared by using the ARL solutions such that the NIE method determines the number of division points $m = 1,000$. ARL_0 of 370 is used for the experiments with the classical and modified EWMA control charts and the AR(1) process; a lower ARL value signifies better effective detection. For the in-control process, the initial parameter values $\beta_0 = 1$, $u = 1$, $X_0 = 1$ as this process mean are determined. In addition, the process mean is tested with shift sizes (δ) of 0.01, 0.02, 0.03, 0.04, 0.05, 0.06, 0.08, 0.10, 0.20, 0.30, 0.40, 0.50, 0.60, 0.80 and 1.00. The optimization procedure in Fig. 1 can be summarized as follows:

Step 1: Specify λ , ϕ , η , r and ARL_0 .

Step 2: Determine the initial values of the process mean on an exponential distribution as: β_0 , u , X_0 .

Step 3: Compute b when a is known by using Eq. (13) for the explicit formula or Eq. (18) for the NIE method.

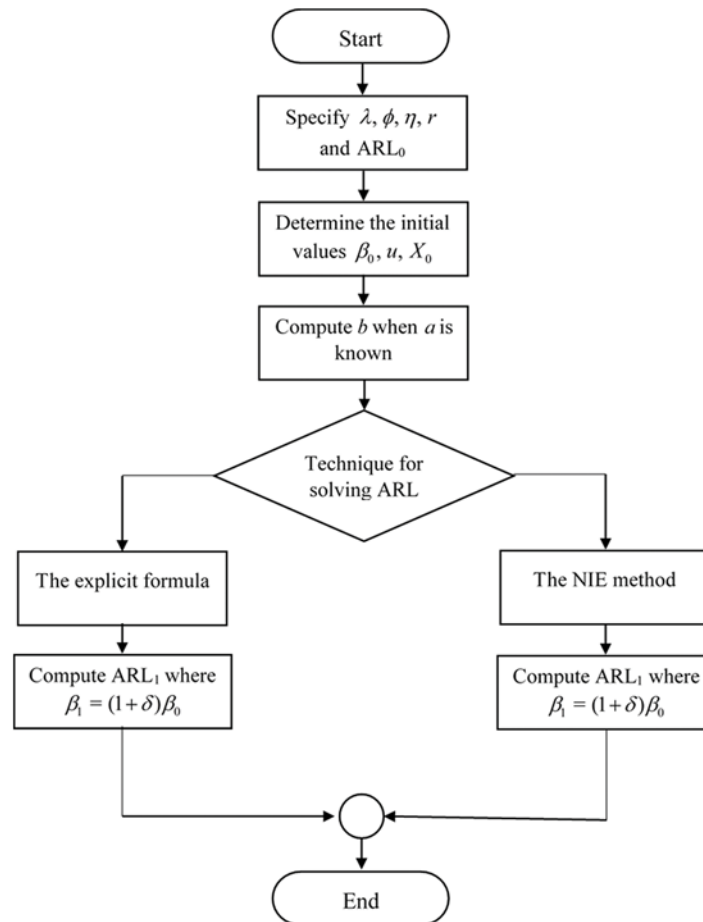


Figure 1: The summarized processing diagram

Step 4: Compute ARL_1 from the b solution in Step 3 by shifting mean (δ) where $\beta_1 = (1 + \delta) \beta_0$.

The efficiency comparison of the ARL between the explicit formula and the NIE method is measured using the absolute relative change (ARC) [33] which can be calculated as:

$$ARC (\%) = \left| \frac{L(u) - L_{NIE}(u)}{L(u)} \right| \times 100\%. \tag{19}$$

Table 1: Comparison of ARL values on the modified EWMA control chart with the AR(1) model using explicit formulas against the NIE method given $\lambda = 0.05$, $\eta = 2$, $r = 1$, $a = 0$ at $\phi = 0.1$ ($b = 0.333987011$), $\phi = -0.1$ ($b = 0.408730497$) for $ARL_0 = 370$

Shift size (δ)	$\phi = 0.1$			$\phi = -0.1$		
	Explicit (CPU time)	NIE (CPU time)	ARC (%)	Explicit (CPU time)	NIE (CPU time)	ARC (%)
0.00	370.00008812 (<0.001)	370.00008589 (9.281)	6.03×10^{-07}	370.00004893 (<0.001)	370.00004557 (9.359)	9.08×10^{-07}
0.01	78.37858370 (<0.001)	78.37858335 (8.969)	4.11×10^{-07}	82.65057512 (<0.001)	82.65057456 (9.312)	6.78×10^{-07}
0.02	43.82837788 (<0.001)	43.82837770 (10.313)	4.11×10^{-07}	46.53183718 (<0.001)	46.53183689 (10.453)	6.23×10^{-07}
0.03	30.42557907 (<0.001)	30.42557895 (9.281)	3.94×10^{-07}	32.39371610 (<0.001)	32.39371591 (9.328)	5.87×10^{-07}
0.04	23.30847758 (<0.001)	23.30847749 (10.468)	3.86×10^{-07}	24.85646420 (<0.001)	24.85646406 (10.328)	5.63×10^{-07}
0.05	18.89793321 (<0.001)	18.89793314 (9.344)	3.70×10^{-07}	20.17481918 (<0.001)	20.17481907 (9.547)	5.45×10^{-07}
0.06	15.89855292 (<0.001)	15.89855286 (10.438)	3.77×10^{-07}	16.986143197 (<0.001)	16.986143105 (10.156)	5.42×10^{-07}
0.08	12.08490680 (<0.001)	12.08490676 (9.406)	3.31×10^{-07}	12.925534561 (<0.001)	12.925534495 (9.500)	5.11×10^{-07}
0.10	9.765566083 (<0.001)	9.765566052 (9.562)	3.17×10^{-07}	10.452061817 (<0.001)	10.452061767 (9.468)	4.78×10^{-07}
0.20	5.090970157 (<0.001)	5.090970145 (10.392)	2.36×10^{-07}	5.453366997 (<0.001)	5.453366978 (10.515)	3.48×10^{-07}
0.30	3.554052055 (<0.001)	3.554052049 (9.546)	0.69×10^{-07}	3.802097396 (<0.001)	3.802097385 (9.500)	2.89×10^{-07}
0.40	2.807071681 (<0.001)	2.807071677 (10.063)	1.42×10^{-07}	2.996034011 (<0.001)	2.996034005 (10.422)	2.00×10^{-07}
0.50	2.373151393 (<0.001)	2.373151390 (9.515)	1.26×10^{-07}	2.525809691 (<0.001)	2.525809687 (9.391)	1.58×10^{-07}
0.60	2.093319852 (<0.001)	2.093319850 (10.219)	9.55×10^{-08}	2.221328911 (<0.001)	2.221328908 (10.109)	1.35×10^{-07}
0.80	1.759313098 (<0.001)	1.759313097 (10.500)	5.68×10^{-08}	1.855915275 (<0.001)	1.855915274 (10.079)	5.39×10^{-08}
1.00	1.570797672 (<0.001)	1.570797671 (9.657)	6.37×10^{-08}	1.648205459 (<0.001)	1.648205458 (9.484)	6.07×10^{-08}

In addition, the speed test results are computed by the CPU time (PC System: Windows 10 Education, i7-6500U CPU@2.50 GHz Processor, 8.00 GB RAM, 64-bit Operating System) in seconds.

Table 2: Comparison of the ARL values between the CUSUM, the classical EWMA and modified EWMA control charts given $\lambda = 0.05$, $\eta = 2$, $a = 0$ at $ARL_0 = 370$

ϕ	Shift size (δ)	CUSUM ($q = 4$)	EWMA ($r = 0$)	Modified EWMA		
				Adjusted $r = 0.5$	Basic $r = 1$	Adjusted $r = 2$
		$(b = 5.45278)$	$(b = 1.145388 \times 10^{-8})$	$(b = 0.150278601)$	$(b = 0.301950105)$	$(b = 0.604752895)$
0.2	0.00	370.000	370.000	370.000	370.000	370.000
	0.01	338.746	297.174	134.052	76.388	53.985
	0.02	310.682	239.724	80.967	42.581	29.372
	0.03	285.440	194.207	57.568	29.521	20.296
	0.04	262.698	157.991	44.414	22.599	15.576
	0.05	242.174	129.058	35.997	18.313	12.684
	0.06	223.623	105.850	30.157	15.401	10.731
	0.08	191.601	72.056	22.602	11.701	8.262
	0.10	165.199	49.824	17.945	9.452	6.768
	0.20	85.904	9.981	8.493	4.926	3.761
	0.30	50.819	3.130	5.435	3.442	2.765
	0.40	33.462	1.617	3.992	2.722	2.275
	0.50	24.017	1.210	3.180	2.304	1.987
	0.60	18.436	1.081	2.673	2.036	1.799
	0.80	12.507	1.017	2.091	1.716	1.570
	1.00	9.553	1.005	1.780	1.536	1.437
RMI		15.058	3.955	1.411	0.481	0.168
		$(b = 4.150138)$	$(b = 1.70872 \times 10^{-8})$	$(b = 0.225127154)$	$(b = 0.452229145)$	$(b = 0.905706536)$
-0.2	0.00	370.000	370.000	370.000	370.000	370.000
	0.01	345.684	298.349	145.780	84.954	60.565
	0.02	323.398	241.604	89.916	48.004	33.268
	0.03	302.945	196.471	64.581	33.470	23.068
	0.04	284.146	160.426	50.138	25.705	17.735
	0.05	266.843	131.521	40.817	20.876	14.456
	0.06	250.895	108.251	34.313	17.584	12.238
	0.08	222.579	74.193	25.848	13.388	9.427
	0.10	198.341	51.632	20.599	10.830	7.722
	0.20	118.297	10.600	9.850	5.654	4.277
	0.30	76.717	3.336	6.325	3.940	3.128
	0.40	53.181	1.692	4.643	3.101	2.558
	0.50	38.902	1.240	3.687	2.611	2.220
	0.60	29.728	1.095	3.084	2.293	1.998
	0.80	19.212	1.020	2.385	1.910	1.725
	1.00	13.717	1.006	2.005	1.692	1.565
RMI		18.278	3.487	1.498	0.539	0.211

The performance comparison of the explicit formula and the NIE method is explained with the ARL, the ARC and the CPU time (Tab. 1). The first results indicate that the ARL values of

the explicit formula are similar to those of the NIE method according to the ARC criterion such that ARC solutions are very low and converge to 0. For the CPU time for calculating the ARL, the explicit formula is faster than the NIE method by around 9 s.

The performance of the modified EWMA control chart on varying scales of constant r , different bound control limits $[a, b]$ and various λ are further tested by using the relative mean index (RMI) [34] which can be written as:

$$RMI = \frac{1}{n} \sum_{i=1}^n \left[\frac{ARL_i(c) - ARL_i(s)}{ARL_i(s)} \right] \tag{20}$$

where $ARL_i(c)$ is the ARL of the control chart for the shift size of row i , $ARL_i(s)$ is the smallest ARL of all of the control charts on row i and the RMI value is smaller, then the control chart has more performance for detecting shifts.

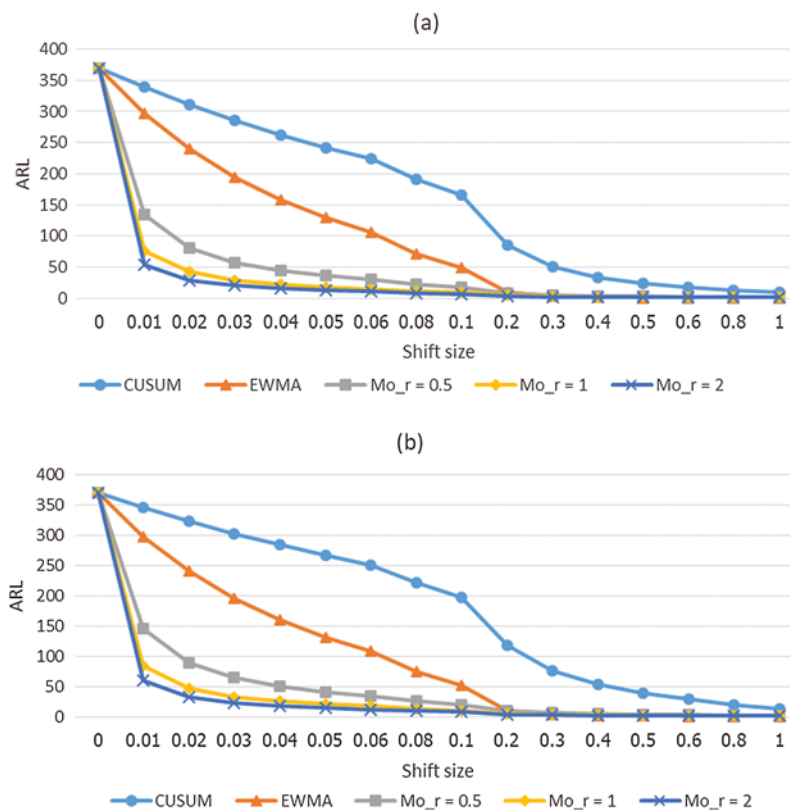


Figure 2: Plot of the CUSUM, the classical EWMA and modified EWMA control charts given (a) $\phi = 0.2$ and (b) $\phi = -0.2$

The CUSUM, the classical EWMA ($r = 0$), the classical modified EWMA ($r = 1$) and the modified EWMA control charts with adjusted $r = 0.5$ and $r = 2$ measured a capability by using the ARL and the RMI at $\phi = 0.2, -0.2$ for $ARL_0 = 370$ are compared and reported in Tab. 2 and Fig. 2. When the process mean is shifted, the ARL results of the modified EWMA control charts have abrupt decrease and lower values in small and intermediate shifts. For large shifts,

the classical EWMA chart is obtained the least ARL. Therefore, the performance of modified EWMA control charts is better than the classical EWMA scheme for small and intermediate shifts. Moreover, the results show that the CUSUM chart has lower performance than modified EWMA control charts for all levels of shifts. From ARL and RMI comparisons, the modified EWMA control charts with higher r values are more effective.

Table 3: Comparison of the ARL values on the modified EWMA control chart with difference control bounds given $\lambda = 0.05$, $\eta = 2$, $r = 1$ at $ARL_0 = 370$

ϕ	Shift size (δ)	$a = 0$	$a = 0.1$	$a = 0.3$	$a = 0.4$
		$(b = 0.273008016)$	$(b = 0.374461655)$	$(b = 0.57735612)$	$(b = 0.67879871)$
0.3	0.00	370.000	370.000	370.000	370.000
	0.01	74.484	69.483	60.267	56.043
	0.02	41.394	38.391	32.967	30.528
	0.03	28.663	26.553	22.770	21.079
	0.04	21.926	20.317	17.440	16.158
	0.05	17.760	16.469	14.165	13.140
	0.06	14.930	13.860	11.951	11.101
	0.08	11.338	10.552	9.148	8.523
	0.10	9.157	8.544	7.450	6.962
	0.20	4.771	4.509	4.037	3.825
	0.30	3.336	3.186	2.914	2.790
	0.40	2.642	2.544	2.365	2.283
	0.50	2.240	2.171	2.045	1.986
	0.60	1.982	1.931	1.837	1.793
	0.80	1.676	1.645	1.587	1.560
	1.00	1.504	1.484	1.445	1.427
RMI		0.232	0.168	0.052	0
		$(b = 0.500416482)$	$(b = 0.603072843)$	$(b = 0.80836715)$	$(b = 0.911008116)$
-0.3	0.00	370.000	370.000	370.000	370.000
	0.01	87.389	81.769	71.317	66.487
	0.02	49.572	46.055	39.668	36.781
	0.03	34.619	32.105	27.577	25.546
	0.04	26.612	24.674	21.196	19.641
	0.05	21.626	20.059	17.254	16.001
	0.06	18.224	16.916	14.577	13.534
	0.08	13.884	12.913	11.178	10.404
	0.10	11.236	10.474	9.110	8.501
	0.20	5.869	5.533	4.927	4.654
	0.30	4.087	3.890	3.532	3.370
	0.40	3.214	3.083	2.843	2.733
	0.50	2.702	2.608	2.436	2.356
	0.60	2.370	2.299	2.168	2.108
	0.80	1.968	1.924	1.842	1.804
	1.00	1.739	1.709	1.652	1.626
RMI		0.238	0.173	0.054	0

For [Tab. 3](#), the ARL results with $ARL_0 = 370$ show the performance of the modified EWMA control chart on various bound control limits $[a, b]$ for $\phi = 0.3, -0.3$ and $a = 0, 0.1, 0.3, 0.4$. The RMI values of the lower bound $a = 0.4$ are 0. When the lower bound (a) is higher, then the modified EWMA control chart can detect better shifts when comparing the ARL and the RMI values in one direction.

Table 4: Comparison of the ARL values on the modified EWMA control chart with various λ given $\eta = 2, r = 1, a = 0.4$ at $ARL_0 = 370$

ϕ	Shift size (δ)	$\lambda = 0.01$	$\lambda = 0.05$	$\lambda = 0.10$	$\lambda = 0.20$
		$(b = 0.672828274)$	$(b = 0.67879871)$	$(b = 0.686452008)$	$(b = 0.702326332)$
0.3	0.00	370.000	370.000	370.000	370.000
	0.01	58.170	56.043	53.700	49.853
	0.02	31.757	30.528	29.182	26.993
	0.03	21.934	21.079	20.146	18.632
	0.04	16.808	16.158	15.448	14.299
	0.05	13.662	13.140	12.571	11.649
	0.06	11.535	11.101	10.627	9.861
	0.08	8.844	8.523	8.172	7.605
	0.10	7.215	6.962	6.686	6.240
	0.20	3.940	3.825	3.700	3.498
	0.30	2.859	2.790	2.715	2.592
	0.40	2.331	2.283	2.231	2.147
	0.50	2.022	1.986	1.948	1.885
	0.60	1.821	1.793	1.763	1.714
0.80	1.578	1.560	1.540	1.508	
1.00	1.440	1.427	1.412	1.388	
RMI		0.118	0.088	0.0542	0
		$(b = 0.897887577)$	$(b = 0.911008116)$	$(b = 0.92785533)$	$(b = 0.962983493)$
-0.3	0.00	370.000	370.000	370.000	370.000
	0.01	68.657	66.487	64.109	60.251
	0.02	38.078	36.781	35.370	33.100
	0.03	26.460	25.546	24.553	22.962
	0.04	20.343	19.641	18.880	17.662
	0.05	16.568	16.001	15.387	14.404
	0.06	14.008	13.534	13.021	12.200
	0.08	10.758	10.404	10.020	9.407
	0.10	8.782	8.501	8.198	7.713
	0.20	4.784	4.654	4.513	4.288
	0.30	3.450	3.370	3.283	3.143
	0.40	2.789	2.733	2.672	2.575
	0.50	2.398	2.356	2.310	2.237
	0.60	2.141	2.108	2.072	2.014
0.80	1.826	1.804	1.779	1.740	
1.00	1.642	1.626	1.608	1.579	
RMI		0.106	0.078	0.048	0

Moreover, the modified EWMA control chart is compared for various $\lambda = 0.01, 0.05, 0.10$ and 0.20 at $ARL_0 = 370$, $a = 0.4$ and $\phi = 0.3, -0.3$ (Tab. 4). The RMI values of $\lambda = 0.20$ are 0. The ARL and the RMI results show that more λ values affect for increasing a detected performance of the modified EWMA control chart.

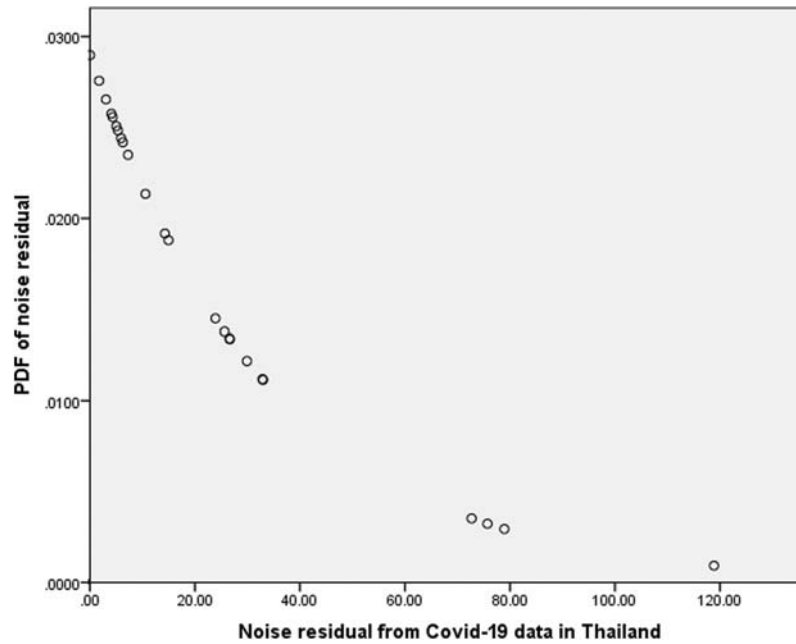


Figure 3: Plot of the noise residual of COVID-19 data in Thailand

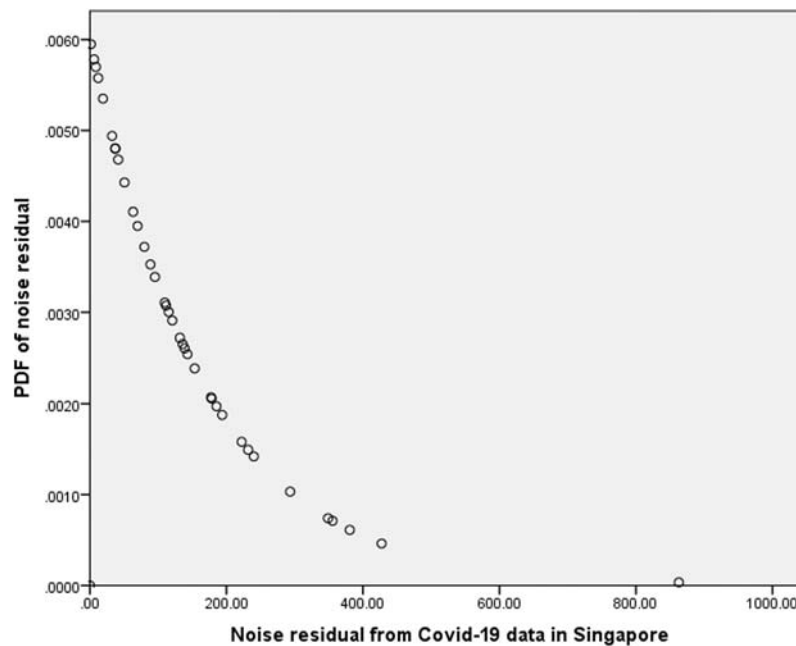


Figure 4: Plot of the noise residual of COVID-19 data in Singapore

7 Application to Real Data

As an example, the modified EWMA control chart is applied to COVID-19 data in Thailand and Singapore [35,36] such that the 100 days of newly infected cases are studied when the more summation of 100 cases. These data are checked to a suitable AR(1) process with an exponential white noise at parameters of COVID-19 data in Thailand $\beta_0 = 34.78$, $\eta = 10.06$, $\phi = 0.664$ and Singapore $\beta_0 = 159.47$, $\eta = 48.99$, $\phi = 0.863$. Moreover, their error term have be tested an exponential distribution and plotted graphs in Figs. 3 and 4, respectively.

Table 5: Comparison of ARL values between the CUSUM, the classical EWMA and modified EWMA control charts for COVID-19 data in Thailand with $\beta_0 = 34.78$, $\eta = 10.06$, $\phi = 0.664$, $a = 0$ at $\lambda = 0.05$ and $ARL_0 = 370$

Shift size (δ)	CUSUM ($q = 100$)	EWMA ($r = 0$)	Modified EWMA		
			Adjusted $r = 0.5$	Basic $r = 1$	Adjusted $r = 2$
	$(b = 167.3)$	$(b = 1.386 \times 10^{-6})$	$(b = 18.5648)$	$(b = 37.2657)$	$(b = 74.6315)$
0.00	370	370	370	370	370
0.01	343.476	300.868	180.287	113.091	83.291
0.02	319.132	245.645	118.387	66.819	47.287
0.03	296.959	201.362	87.706	47.459	33.189
0.04	276.733	165.712	69.400	36.826	25.669
0.05	258.253	136.898	57.248	30.105	20.993
0.06	241.345	113.522	48.602	25.475	17.805
0.08	211.636	78.935	37.134	19.512	13.738
0.10	186.554	55.686	29.889	15.841	11.253
0.20	106.523	12.056	14.660	8.301	6.181
0.30	67.202	3.840	9.494	5.751	4.462
0.40	45.918	1.881	6.971	4.483	3.598
0.50	33.445	1.318	5.507	3.729	3.078
0.60	25.638	1.130	4.566	3.233	2.732
0.80	16.897	1.029	3.452	2.624	2.298
1.00	12.397	1.009	2.828	2.267	2.039
RMI	13.085	2.367	1.797	0.752	0.380

Table 6: Comparison of ARL values between the CUSUM, the classical EWMA and modified EWMA control charts for COVID-19 data in Singapore with $\beta_0 = 159.47$, $\eta = 48.99$, $\phi = 0.863$, $a = 0$ at $\lambda = 0.05$ and $ARL_0 = 370$

Shift size (δ)	CUSUM ($q = 500$)	EWMA ($r = 0$)	Modified EWMA		
			Adjusted $r = 0.5$	Basic $r = 1$	Adjusted $r = 2$
	$(b = 745.43)$	$(b = 5.115 \times 10^{-6})$	$(b = 68.1366)$	$(b = 136.8)$	$(b = 273.966)$
0.00	370	370	370	370	370
0.01	343.887	300.195	169.332	103.606	75.401
0.02	320.094	244.582	108.987	60.300	42.324
0.03	298.381	200.081	79.937	42.565	29.584

(Continued)

Table 6: Continued

Shift size (δ)	CUSUM ($q = 500$)	EWMA ($r = 0$)	Modified EWMA		
			Adjusted $r = 0.5$	Basic $r = 1$	Adjusted $r = 2$
0.04	278.536	164.327	62.867	32.917	22.836
0.05	260.371	135.488	51.644	26.854	18.657
0.06	243.720	112.138	43.711	22.693	15.816
0.08	214.385	77.685	33.255	17.353	12.200
0.10	189.532	54.613	26.691	14.075	9.995
0.20	109.528	11.662	13.006	7.375	5.509
0.30	69.646	3.701	8.408	5.122	3.995
0.40	47.802	1.828	6.175	4.005	3.236
0.50	34.882	1.296	4.886	3.344	2.781
0.60	26.737	1.120	4.062	2.910	2.478
0.80	17.558	1.026	3.089	2.379	2.101
1.00	12.812	1.008	2.549	2.071	1.876
RMI	14.423	2.689	1.697	0.678	0.320

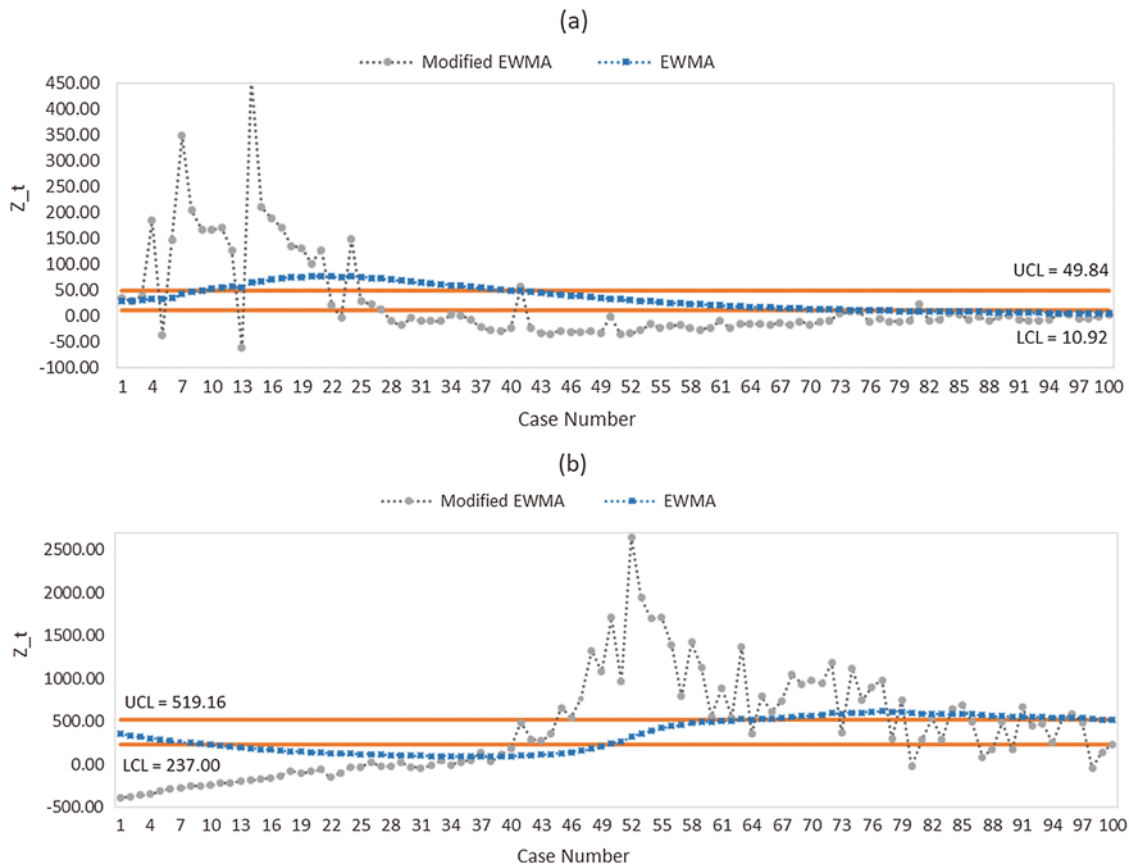


Figure 5: Plot of the classical EWMA and modified EWMA control chart with $r = 2$ for COVID-19 data in (a) Thailand and (b) Singapore

From [Tabs. 5 and 6](#), the results of ARL and the RMI are used to compare the CUSUM, the classical EWMA and modified EWMA control charts with real-world data of COVID-19 data in Thailand and Singapore. The results are in accordance with the simulation data in [Tab. 2](#) and show that the modified EWMA control chart adjusted for high r performs well for small and intermediate level shifts.

In [Fig. 5](#), the modified EWMA control chart with $r = 2$ and the classical EWMA control chart are plotted by calculating Z_t of COVID-19 data in Thailand and Singapore at the exponential smoothing parameter $\lambda = 0.05$ with the optimal control width limit of EWMA chart $L = 2.615$ [37] and the calculated control width limit of the modified EWMA chart $L_m = 0.204$ at bound control limits of Thailand [10.92, 49.84] and bound control limits of Singapore [519.16, 237]. The results show that Z_t values of the modified EWMA control chart with $r = 2$ exceed the bound since the 4th observation, while Z_t values of the classical EWMA control chart are the out-of-control limit at the 9th observation for Thailand. In Singapore, Z_t values of the modified EWMA control chart with $r = 2$ exceed the bound since the first observation, while the classical EWMA control chart signals an alarm in the 10th observation. Therefore, the modified EWMA control chart can detect shifts more quickly than the classical EWMA control chart.

8 Discussion and Conclusions

The performance of a control chart can be evaluated by using the ARL. In this paper, the explicit formula and the numerical integral equation (NIE) method of ARL solutions are established on a two-sided modified EWMA control chart for an AR(1) process with an exponential white noise. The ARL results of both methods are computed and their performances compared via the ARC and the CPU time. The explicit formula shows the actual values of the ARL and is faster calculation than the NIE approach. Moreover, the ARL and RMI results are compared between the CUSUM, the classical and modified EWMA control charts with various r , for which the latter provides better detection for small and intermediate shifts. Next, the performance of the modified EWMA control chart is tested on various bound control limits and is found to be better for higher upper bound values. In addition, this model is applied to the real-world data (COVID-19 data in Thailand and Singapore), with which it obtains similar results as with the simulated data; this result supports the excellent performance of the modified EWMA control chart. In future research, we will establish the optimal bound control limits of the modified EWMA control chart and hope to extend our approach to many new control charts currently under development for different processes.

Funding Statement: The research was supported by King Mongkut's University of Technology North Bangkok Contract No. KMUTNB-62-KNOW-018.

Conflicts of Interest: The authors declare that they have no conflicts of interest to report regarding the present study.

References

1. Kovarik, M., Sarga, L., Klimek, P. (2015). Usage of control charts for time series analysis in financial management. *Journal of Business Economics and Management*, 16(1), 138–158. DOI 10.3846/16111699.2012.732106.
2. Ozilgen, S. (2011). Statistical quality control charts: New tools for studying the body mass index of populations from the young to the elderly. *Journal of Nutrition, Health & Aging*, 15(5), 333–334. DOI 10.1007/s12603-010-0290-8.

3. Poovarasan, R., Keerthi, S., Yuvashree, K., Thirumalai, C. (2018). Analysis on diabetes patients using Pearson, cost optimization, control chart. *Proceedings of the International Conference on Trends in Electronics and Informatics*, vol. 1, pp. 1139–1142. DOI 10.1109/ICOEI.2017.8300891.
4. Montgomery, D. C. (2013). *Introduction to statistical quality control*. New Jersey: John Wiley & Sons.
5. Roberts, W. S. (1959). Control chart tests based on geometric moving averages. *Technometrics*, 1(3), 239–250. DOI 10.1080/00401706.1959.10489860.
6. Page, E. S. (1954). Continuous inspection schemes. *Biometrika*, 41(1–2), 100–115. DOI 10.1093/biomet/41.1-2.100.
7. Patel, A. K., Divecha, J. (2011). Modified exponentially weighted moving average (EWMA) control chart for an analytical process data. *Journal of Chemical Engineering and Materials Science*, 2, 12–20. DOI 10.1088/1742-6596/979/1/012097.
8. Khan, N., Aslam, M., Jun, C. H. (2017). Design of a control chart using a modified EWMA statistic. *Quality and Reliability Engineering International*, 33(5), 1095–1104. DOI 10.1002/qre.2102.
9. Khusna, H., Mashuri, M., Suhartono, S., Prastyo, D. D., Ahsan, M. (2018). Multioutput least square SVR-based multivariate EWMA control chart: The performance evaluation and application. *Cogent Engineering*, 5(1), 1–14. DOI 10.1080/23311916.2018.1531456.
10. Flury, M. I., Quaglino, M. B. (2018). Multivariate EWMA control chart with highly asymmetric gamma distributions. *Quality Technology & Quantitative Management*, 15(2), 230–252. DOI 10.1080/16843703.2016.1208937.
11. Chananet, C., Areepong, Y., Sukparungsee, S. (2015). A markov chain approach for average run length of EWMA and CUSUM control chart based on ZINB Model. *International Journal of Applied Mathematics and Statistics*, 53(1), 126–137. Available: <http://www.ceser.in/ceserp/index.php/ijamas/article/view/3385>.
12. Sukparungsee, S. (2012). Combining martingale and integral equation approaches for finding optimal parameters of EWMA. *Applied Mathematical Sciences*, 6, 4471–4482.
13. Suriyakit, W., Areepong, Y., Sukparungsee, S., Mititelu, G. (2012). On EWMA procedure for AR(1) observations with exponential white noise. *International Journal of Pure and Applied Mathematics*, 77, 73–83.
14. Busaba, J., Sukparungsee, S., Areepong, Y. (2012). Numerical approximations of average run length for AR(1) on exponential CUSUM. *Proceedings of the International MultiConference of Engineers and Computer Scientists*, vol. 2, pp. 1268–1273.
15. Petcharat, K., Sukparungsee, S., Areepong, Y. (2015). Exact solution of the average run length for the cumulative sum chart for a moving average process of order q. *ScienceAsia*, 41(2), 141–147. DOI 10.2306/scienceasia1513-1874.2015.41.141.
16. Peerajit, W., Areepong, Y., Sukparungsee, S. (2018). Numerical integral equation method for ARL of CUSUM chart for long-memory process with non-seasonal and seasonal ARFIMA models. *Thailand Statistician*, 16(1), 26–37.
17. Sukparungsee, S., Areepong, Y. (2017). An explicit analytical solution of the average run length of an exponentially weighted moving average control chart using an autoregressive model. *Chiang Mai Journal of Science*, 44(3), 1172–1179.
18. Sunthornwat, R., Areepong, Y., Sukparungsee, S. (2017). Average run length of the long-memory autoregressive fractionally integrated moving average process of the exponential weighted moving average control chart. *Cogent Mathematics*, 4(1), 1–11. DOI 10.1080/23311835.2017.1358536.
19. Sunthornwat, R., Areepong, Y., Sukparungsee, S. (2018). Average run length with a practical investigation of estimating parameters of the EWMA control chart on the long memory AFRIMA process. *Thailand Statistician*, 16(2), 190–202.
20. Peerajit, W., Areepong, Y., Sukparungsee, S. (2019). Explicit analytical solutions for ARL of CUSUM chart for a long-memory SARFIMA model. *Communications in Statistics–Simulation and Computation*, 48(4), 1176–1190. DOI 10.1080/03610918.2017.1408821.
21. Vanhatalo, E., Kulahci, M. (2014). The effect of autocorrelation on the Hotelling T^2 control chart. *Quality and Reliability Engineering International*, 31(8), 1779–1796. DOI 10.1002/qre.1717.

22. He, Z., Wang, Z., Tsung, F., Shang, Y. (2016). A control scheme for autocorrelated bivariate binomial data. *Computers and Industrial Engineering*, 98, 350–359. DOI 10.1016/j.cie.2016.06.001.
23. Kim, H., Lee, S. (2017). On first-order integer-valued autoregressive process with Katz family innovations. *Journal of Statistical Computation and Simulation*, 87(3), 546–562. DOI 10.1080/00949655.2016.1219356.
24. Yadav, V., Nath, S. (2017). Forecasting of PM₁₀ using autoregressive models and exponential smoothing technique. *Asian Journal of Water, Environment and Pollution*, 14(4), 109–113. DOI 10.3233/AJW-170041.
25. Shapoval, A., Mouel, J. L. L., Shnirman, M., Courtillot, V. (2015). Stochastic description of the high-frequency content of daily sunspots and evidence for regime changes. *Astrophysical Journal*, 799(1), 1–8. DOI 10.1088/0004-637X/799/1/56.
26. Hirsch, S., Hartmann, M. (2014). Persistence of firm-level profitability in the European dairy processing industry. *Agricultural Economics*, 45(1), 53–63. DOI 10.1111/agec.12129.
27. Andel, J. (1988). On AR(1) processes with exponential white noise. *Communications in Statistics–Theory and Methods*, 17(5), 1481–1495. DOI 10.1080/03610928808829693.
28. Fellag, H., Ibazizen, M. (2001). Estimation of the first-order autoregressive model with contaminated exponential white noise. *Journal of Mathematical Sciences*, 106(1), 2652–2656. DOI 10.1023/A:1011318515549.
29. Pereira, I., Amaral-Turkman, M. A. (2004). Bayesian prediction in threshold autoregressive models with exponential white noise. *Test*, 13(1), 45–64. DOI 10.1007/BF02603000.
30. Champ, C. W., Rigdon, S. E. (1991). A comparison of the Markov Chain and the integral equation approaches for evaluating the run length distribution of quality control charts. *Communication in Statistics–Simulation*, 20(1), 191–203. DOI 10.1080/03610919108812948.
31. Davison, K. R., Donsig, A. P. (2010). *Real analysis with real applications*. New York: Springer-Verlag.
32. Phanthuna, P., Areepong, Y., Sukparungsee, S. (2018). Numerical integral equation methods of average run length on modified EWMA control chart for exponential AR(1) process. *Proceedings of the International MultiConference of Engineers and Computer Scientists*, vol. 2, pp. 845–847.
33. Nguyen, Q. T., Tran, K. P., Castagliola, P., Celano, G., Lardjane, S. (2019). One-sided synthetic control charts for monitoring the multivariate coefficient of variation. *Journal of Statistical Computation and Simulation*, 89(10), 1841–1862. DOI 10.1080/00949655.2019.1600694.
34. Tang, A., Castagliola, P., Sun, J., Hu, X. (2018). Optimal design of the adaptive EWMA chart for the mean based on median run length and expected median run length. *Quality Technology and Quantitative Management*, 16(4), 439–458. DOI 10.1080/16843703.2018.1460908.
35. WHO (2020). Thailand situation reports: Coronavirus disease (COVID-19) dashboard. <https://covid19.who.int/region/wpro/country/sg>.
36. WHO (2020). Singapore situation reports: Coronavirus disease (COVID-19) dashboard. <https://covid19.who.int/region/searo/country/th>.
37. Lucas, J. M., Saccucci, M. S. (1990). Exponentially weighted moving average control schemes: Properties and enhancements. *Technometrics*, 32(1), 1–12. DOI 10.1080/00401706.1990.10484583.